MULTIFRACTAL FEATURE DESCRIPTOR FOR DIAGNOSING LIVER AND PROSTATE CANCERS IN H&E STAINED HISTOLOGIC IMAGES

C. Atupelage[⋆], *H. Nagahashi*[†], *M. Yamaguchi*[⋆†], *T. Abe*[††], *A. Hashiguchi*[††], *M. Sakamoto*[††]

[⋆]Department of Computational Intelligence and Systems Science, Tokyo Institute of Technology, Japan.
[†]Imaging Science and Engineering Laboratory, Tokyo Institute of Technology, Japan.
[⋆†]Global Scientific Information and Computing Center, Tokyo Institute of Technology, Japan.
[††]Department of Pathology, School of Medicine, Keio University, Japan.

ABSTRACT

Histologic imaging plays an important role in discriminating cancerous tissues of several body organs. However, the human histopathological examinations may be subjective and error prone, because of the complexity of the appearances of the histologic texture. These limitations can be overcome by adopting quantitative computational methods with human histopathological examination routines. This study proposes a new feature descriptor to characterize texture of histologic images. The proposed method derives a discriminative feature space by observing the self-similarity characteristics of the texture based on fractal geometry. The merit of utilizing fractal geometry to describe the histologic texture is assessed by a classification experiment. The experimental results indicate that the proposed feature descriptor can classify cancer and non-cancer tissues of histologic images of liver and prostate images around 95% of correct classification rate.

Index Terms— Histology, Fractal, Multifractal, Feature descriptors, Classification

1. INTRODUCTION

The word "Cancer" is a generic term for group of diseases and it may be confirmed by a histopathological examination of the suspected body tissues. In a histopathologic examination, pathologist investigates some specific structural changes of the tissues, and determine the malignancies according to the divergence of the structures from their healthy state. These decisions may be influenced by several circumstances such as pathologists' personal experiences, quality of the equipments, etc. However, quantitative computational techniques can be utilized to overcome the inconsistencies of consequences of human diagnosing.

In this paper, we propose a new textural feature descriptor, which transforms a given texture into a discriminative feature space by observing self-similarity characteristics of the texture. Multifractal analysis is used to compute the self-similarity of the natural images. The multifractal computation is comprised of a function called *multifractal measure*. The proposed feature descriptor utilizes six-multifractal measures and constructs six-dimensional feature space for a given texture. Subsequently, the derived feature space is employed with a classification framework to distinguish cancer and non-cancer tissues of hitologic images of two body organs; liver and prostate. The outcome of the classification is summarized by computing the correct classification rate.

This research is supported by New Energy and Industrial Technology Development Organization (NEDO) in Japan under the research and development project of Pathological Image Recognition.

2. FRACTAL AND MULTIFRACTAL FUNDAMENTALS

Fractal structure is a geometric shape which can be iteratively fragmented into small components and each component has approximately or exactly similar shape to its immediate origin. This property is called self-similarity. The statistical quantity that we used to compute the self-similarity of a structure is called fractal dimension. For further information of fractal dimension, please refer to [1]. Among several fractal dimension estimation algorithms, the *Box-Counting* method [2] is widely used because of its less computational cost, high accuracy and easy implementation. The Box Counting algorithm involves covering a structure:S by a grid of boxes of side length:ε and counting the number of non-empty boxes:$N_\varepsilon(S)$. The Box counting dimension (fractal dimension):D_B of S is computed by,

$$D_B = -\lim_{\varepsilon \to 0} \frac{\log N_\varepsilon(S)}{\log(\varepsilon)} \tag{1}$$

Generally, fractals are deterministic. To the contrary, random structures or natural images are non-deterministic. Therefore, a single fractal dimension may not be adequate to observe the self-similarity of natural images. The self-similarity of such structure is characterized by spectrum of fractals known as multifractals [3]. Multifractal computation for natural images is carried out in two stages. At first; one

may find non-integer exponent:α by utilizing a particular multifractal measure, μ as defined in equation 2.

$$\alpha = \lim_{\varepsilon \to 0} \frac{\log(\mu(S'))}{\log(\varepsilon)} \tag{2}$$

where, S' stands for the squared region of size $\varepsilon \times \varepsilon$.

The α describes the point-wise local irregularity of the structure. It is intuitive that same or similar α may be distributed randomly in the entire structure. At the second step, one may derive a sub-structure from the localization of similar α values and estimate the fractal dimension by using the box counting method. In this manner, the range of α from minimum to maximum can be quantized into groups and each group can be utilized to derive a sub-structure. By finding the fractal dimension of each sub-structures we obtain spectrum of fractal dimensions called *multifractal spectrum*:$f(\alpha)$. The multifractal spectrum provide global regularity information of the structure.

In the multifractal computation, we can obtain α and $f(\alpha)$ values correspond to each of the pixels in the reference image. More precisely, a given image can be transformed into two domains; α and $f(\alpha)$ feature domains.

3. METHODOLOGY

3.1. Multifractal feature extraction

Multifractal feature domain provides some kind of textural information, which may not be observable in gray-scale domain. Additionally, by employing different multifractal measures one may observe textural information from different viewpoints. We utilized 6 multifractal measure to compute α and $f(\alpha)$ features in order to form 6-dimensional feature spaces for α and $f(\alpha)$ respectively. Among the multifractal measures defined in [4], we empirically selected three measures called *Maximum*:μ_{Max}, *Minimum*:μ_{Min} and *Summation*:μ_{Sum}, and their definitions are given in equations (3a), (3b) and (3c) respectively. We derived another measure based on differential box counting algorithm [2] to obtain the normalized difference between maximum and minimum gray values, which we call *NDiff*:μ_{nDiff} and the definition is given in the equation (3d). Additionally, we use other two measures called *Gradient Magnitude*:μ_{GM} and *Gradient Angle*:μ_{GA} from the gradient information of the image by following the definition in [5]. The definitions of μ_{GM} and μ_{GA} have been given in equations (3e) and (3f) respectively. In figure 1, we have shown the appearance of α and $f(\alpha)$ derived for each multifractal measure.

$$\mu_{Max} = \underset{(k,l)\in\Omega}{max}\, g(k,l) \tag{3a}$$

$$\mu_{Max} = \underset{(k,l)\in\Omega^*}{min}\, g(k,l) \tag{3b}$$

$$\mu_{Sum} = \sum_{(k,l)\in\Omega} g(k,l) \tag{3c}$$

$$\mu_{Ndiff} = \left(\underset{(k,l)\in\Omega}{max}\, g(k,l) - \underset{(k,l)\in\Omega^*}{min}\, g(k,l) \right) / i \tag{3d}$$

$$\mu_{GM} = \sqrt{G_x^2 + G_y^2} \tag{3e}$$

$$\mu_{GA} = \tan^{-1}(G_y / G_x) \tag{3f}$$

where $\mu_{(.)}$ is stands for multifractal measure, Ω is a square region of side length i, Ω^* represents all non-zero pixels in the region Ω, $g(k,l)$ is the gray scale intensity at point (k,l), G_x and G_y are gradient vectors computed at the center of Ω towards x and y directions.

3.2. Classification model

Based on the above observations a given image can be described in multifractal feature domain; α or $f(\alpha)$. In this study, we utilized these feature spaces with a texton dictionary based classification model to classify histologic prostate images. Generally, a universal texton dictionary is a collection of texture primitives, which can be used to dictate any texture. Since to compute universal texton dictionary is impractical, one may defined several constraints for a particular texton dictionary. For an example, a texton dictionary derived from the images captured in 20x magnification can be applied only to the images captured in that magnification. To construct a texton dictionary it is required to find a common texture primitives (feature vectors) for the entire dataset. Therefore, we performed *k*-mean clustering for the entire feature pool, which is constructed by applying the feature descriptor to the every image in the dataset and yielded the texton dictionary from every cluster centroids of each cluster.

In a texton dictionary based classification model, every image in the sample dataset is labeled by using the texton dictionary in some manner. More precisely, for a particular feature vector in the feature space, we find a texton which has the minimal Euclidean distance, and the corresponding pixel is labeled by the index of that texton. This label representation can be yielded a histogram known as texture signature, where each bin stands for the texton's index and its value indicates the number of occurrences of the corresponded label over the entire image. Subsequently, we employed all texture signatures as input vector of the classifier to distinguish cancerous tissue of prostate images.

4. EXPERIMENTS AND RESULTS

The proposed multifractal feature descriptor is assessed by a classification problem. We utilized two types of H&E (Hematoxylin and Eosin) stained biopsy specimens; i)liver and ii)prostate obtained from several cancer patients to construct the sample dataset. Each sample specimen is scanned to whole slide image (WSI) by a scanner called *Nano-Zoomer*[6] using objective lens of 20x magnification.

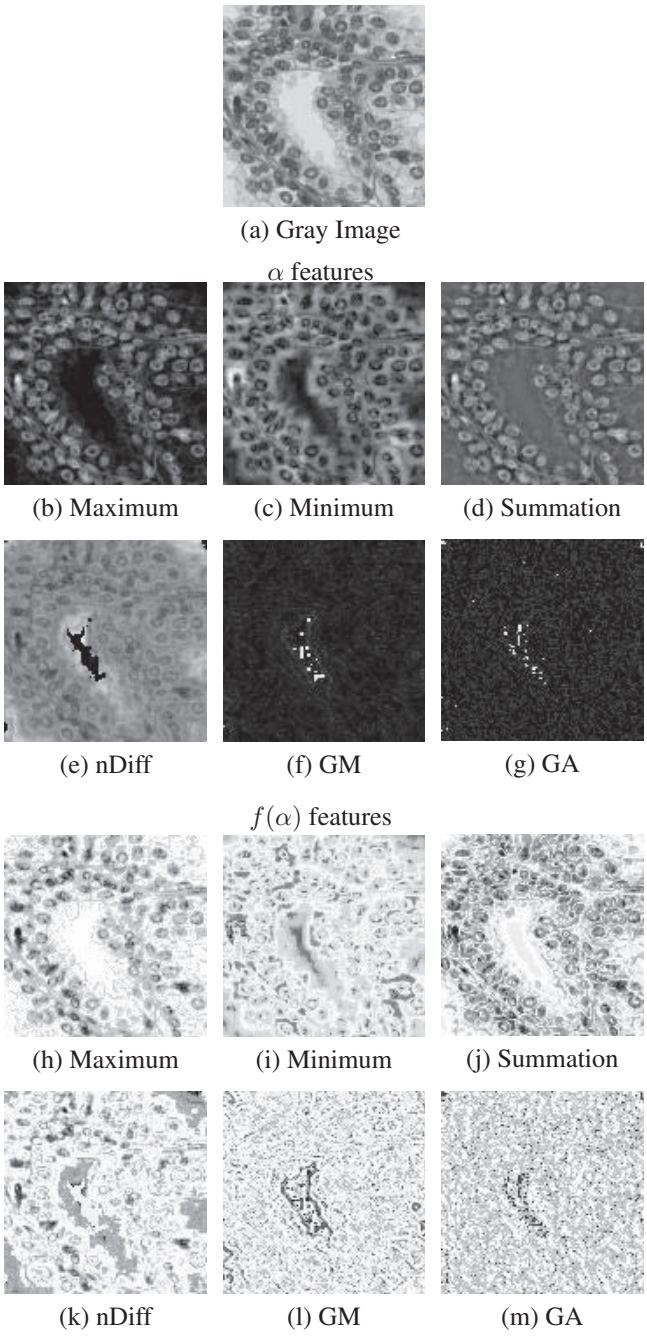


Fig. 1. Visual representation of Multifractal features. (a) sample patch of prostate gray image, (b) to (g) and (h) to (m) present α and $f(\alpha)$ features of (a) respectively. All images have been normalized to grey scale; 0$\sim$255 for clear visualization.

Cancer regions are annotated and confirmed by several experienced pathologists. Each WSI can be visualized in 8-magnifications; 1.25x, 2.5x, 5.0x, 10x, 20x, 40x, 63x, and 100x through a specific tool called *NDPViewer*[6].

The appearance of tissue level components such as nuclei, lumen, cytoplasm, etc., is deviated with the magnification of the digital slider. Moreover, different sizes of cancer regions are erratically distributed over the entire WSI. We defined two parameters to categorize the sample dataset; i)Magnification of the image, and ii)Patch size. As a result, for each organ (liver and prostate) we set up 24 categories of sample datasets; 3 sizes of sample patches (64$\times$64, 128$\times$128 and 256$\times$256 pixels) captured in 8 different magnifications. From each category, we randomly picked 400 sample patches in equal amounts for cancer and non-cancer regions.

In the experiment, we computed the texton dictionaries for each magnification and obtained the texture signatures for each of the image in the datasets. We empirically decided that 300 textons of dictionary is adequate to obtain considerable classification performance in the classifier. The supervised non-parametric classifier called Support Vector Machine (SVM) is used as the classifier and data was elected according to the *k-fold cross validation* method. We defined the evaluation scale as *Correct Classification Rate (CCR)*; the percentage of the number of correct classifications to the total number of samples. Furthermore, to ensure the potentiality of the proposed method, we compared the CCR of our proposed feature extraction method with other two feature descriptors; i) GLOG filters (Gaussian and Laplacian of Gaussian) [7] and, ii) Gabor filters [8]. We used 12 and 16 effective filters for GLOG and Gabor filter banks respectively.

Table 1 and table 2 depict the comparative summary of CCRs for liver and prostate data samples respectively. Due to the space limitation, we present the results of patch sizes 128$\times$128 and 256$\times$256 pixels. The presentation of the results follows the format $x \pm y$, where x and y stand for the mean and standard error of CCRs computed from 10 iterations (10-fold cross validation) respectively. The digital slider visualizes the biopsy sample in different magnifications by interpolating the originally scanned raw data (20x optical lens). Since we found several visual artifacts in the images captured in lager magnifications; 40x to 100x the results of lower magnification are considered to be an important. Therefore, we computed the average (shown as bold texts) for the magnification scales from 1.25x to 20.00x. It is obvious from the table 1 and table 2 that multifractal features descriptor outperforms the other filter-bank based feature descriptors.

The figures in table 1 and table 2 indicate that α features have higher CCR than $f(\alpha)$ features. This is intuitive that $f(\alpha)$ features may loss some tiny information of the texture at the quantization stage of multifractal computation. However, still it can be considered as significant, because it exceed the CCR of comparative feature sets.

5. CONCLUSION

This paper proposed a new multifractal feature descriptor to discriminate the cancer and non-cancer regions of histologic

Table 1. CCRs for liver data samples. GLO and GAB stands for GLOG filters and Gabor filters respectively.

Mag.	128×128				256×256			
Scale	α	$f(\alpha)$	GLO	GAB	α	$f(\alpha)$	GLO	GAB
1.25	95.3 ±1.3	92.3 ±1.5	74.8 ±1.8	82.8 ±2.5	95.5 ±0.3	94.9 ±0.3	89.2 ±1.1	91.5 ±1.3
2.50	94.3 ±1.3	91.8 ±1.6	73.3 ±1.7	89.5 ±2.0	96.5 ±0.8	95.5 ±0.9	82.3 ±1.9	88.4 ±1.4
5.00	96.5 ±1.0	92.0 ±1.7	80.0 ±1.2	85.8 ±1.2	96.3 ±0.9	94.5 ±1.3	83.8 ±1.6	87.5 ±1.5
10.00	93.0 ±2.0	82.0 ±2.2	70.3 ±1.8	77.3 ±1.9	96.8 ±0.9	95.3 ±1.3	82.5 ±1.9	85.6 ±1.7
20.00	77.5 ±1.9	76.8 ±2.4	59.0 ±3.0	71.5 ±1.9	95.7 ±1.7	95.2 ±1.7	65.5 ±2.8	83.8 ±1.8
Avg.	**91.3 ±1.5**	**87.0 ±1.9**	**71.5 ±1.9**	**81.4 ±1.9**	**96.2 ±0.9**	**95.1 ±1.1**	**80.6 ±1.9**	**87.3 ±1.5**
40.00	73.3 ±2.5	66.0 ±2.0	56.0 ±3.0	63.3 ±2.1	94.9 ±1.8	91.9 ±1.9	65.5 ±2.3	78.8 ±2.2
63.00	66.5 ±2.5	59.5 ±2.4	59.0 ±3.5	57.3 ±1.9	85.8 ±2.8	78.3 ±1.9	55.8 ±2.7	69.3 ±2.5
100.0	59.8 ±2.4	56.3 ±2.5	54.3 ±2.7	56.0 ±2.4	67.3 ±2.5	67.0 ±2.3	57.3 ±2.7	63.0 ±2.1

Table 2. CCRs for prostate data samples. GLO and GAB stands for GLOG filters and Gabor filters respectively.

Mag.	128×128				256×256			
Scale	α	$f(\alpha)$	GLO	GAB	α	$f(\alpha)$	GLO	GAB
1.25	94.8 ±0.6	94.4 ±0.9	75.3 ±0.6	93.9 ±1.3	96.9 ±0.3	95.9 ±0.0	90.9 ±1.3	89.7 ±0.6
2.50	95.5 ±0.8	94.3 ±1.1	77.0 ±1.2	93.7 ±1.7	95.8 ±0.3	96.3 ±0.6	87.9 ±1.9	90.7 ±1.2
5.00	96.3 ±2.6	93.5 ±1.8	63.0 ±1.8	94.3 ±1.9	97.5 ±0.8	96.5 ±0.9	86.0 ±1.5	88.8 ±1.8
10.00	96.8 ±1.6	92.5 ±1.8	61.8 ±2.2	90.0 ±1.3	95.8 ±1.1	94.8 ±1.8	73.5 ±2.0	78.5 ±2.2
20.00	91.5 ±0.8	83.3 ±2.8	60.3 ±2.1	80.5 ±2.3	94.9 ±1.7	92.5 ±1.8	69.8 ±2.4	76.0 ±2.1
Avg.	**95.0 ±1.3**	**91.6 ±1.7**	**67.5 ±1.6**	**90.5 ±1.7**	**96.1 ±0.8**	**95.2 ±1.0**	**81.6 ±1.8**	**84.7 ±1.6**
40.00	83.0 ±2.9	82.8 ±2.5	57.5 ±2.5	76.0 ±2.3	92.0 ±2.3	90.3 ±2.3	63.5 ±2.5	68.5 ±2.5
63.00	73.8 ±3.6	69.0 ±2.9	57.0 ±2.3	67.0 ±1.3	78.0 ±2.1	67.0 ±2.1	58.3 ±2.7	63.8 ±2.3
100.0	67.3 ±2.4	67.0 ±2.2	54.0 ±2.4	63.8 ±1.5	75.3 ±2.1	66.3 ±2.4	53.0 ±2.7	66.5 ±2.4

images. In multifractal domain, two-kinds of features can be extracted; local irregularity:α and global regularity$f(\alpha)$. The proposed feature descriptor utilized six multifractal measures to construct the feature spaces for each α and $f(\alpha)$ domains. The significance of utilizing multifractal analysis to describe the histologic texture is investigated by a classification problem. We performed an experiment to distinguish cancer and non-cancer tissues of two types of body organs; liver and prostate. The out come of the classifier is measured as correct classification rate. Furthermore, we utilized two feature descriptors; GLOG and Gabor filters with the same dataset to compare the performance. The experimental results indicate; the multifractal features are more appropriate to characterize histologic texture than the other two feature descriptors. Numerically, α and $f(\alpha)$ features have achieve around 95% of correct classification rate for the image size 256×256 pixels.

Furthermore, the proposed feature descriptor is independent from the morphological characteristics of tissue level component such as nuclei, instead it observes the entire textural information. Therefore, the proposed feature descriptor may be applicable to distinguish cancerous tissues of histologic images of different kind body organs.

6. REFERENCES

[1] B.B. Chaudhuri and N. Sarkar, "Texture segmentation using fractal dimension," *IEEE Transactions on Pattern Analysis and Machine Intelligence*, vol. 17, no. 1, pp. 72–77, 1995.

[2] N Sarkar and B. B. Chaudhuri, "An efficient differential Box-Counting approach to compute fractal dimension of image," *IEEE Transaction on Systems Man and Cybernetics*, vol. 24, no. 1, pp. 115–20, 1994.

[3] I. Reljin, B. Reljin, I. Pavlovic, and I. Rakocevic, "Multifractal analysis of gray-scale images," in *10th Mediterranean Electrotechnical Conference*, 2000, pp. 490–3.

[4] Jacques Lvy Vhel and Pascal Mignot, "Multifractal segmentation of images," in *Fractals 2*, 1994, pp. 379–82.

[5] Antonio Turiel and Nstor Parga, "The multifractal structure of contrast changes in natural images: From sharp edges to textures," *Neural Computation - NECO*, vol. 12, no. 4, pp. 763–93, 2000.

[6] "NanoZoomer 2.0-HT," http://jp.hamamatsu.com/products/life-science/pd267/5103/nzoomb/index_ja.html.

[7] Jitendra Malik and Thomas Leung, "Representing and recognizing the visual appearance of materials appearance of materials using three-dimensional textons," *International Journal of Computer Vision*, pp. 29–44, 2001.

[8] Francesco Bianconi and Antonio Fernndez, "Evaluation of the effects of gabor filter parameters on texture classification," *Journal of Pattern Recognition*, vol. 40, no. 12, 2007.